Materials Research. 2023; 26:e20230190
DOI: https://doi.org/10.1590/1980-5373-MR-2023-0190

Fabrication of Quasicrystalline Scaffolds From the Al-Cu-Fe System by Dynamic Freeze-Casting

Miguel L. Lapér[a], Eduardo H.M. Nunes[a,c], Manuel Houmard[b,c], Witor Wolf[a*]

[a]*Universidade Federal de Minas Gerais, Departamento de Engenharia Metalúrgica e de Materiais, 31270-901, Belo Horizonte, MG, Brasil.*
[b]*Universidade Federal de Minas Gerais, Departamento de Engenharia Química, 31270-901, Belo Horizonte, MG, Brasil.*
[c]*Centro de Tecnologia em Nanomateriais e Grafeno (CTNano), 31310-260, Belo Horizonte, MG, Brasil.*

Received: April 04, 2023; Revised: July 04, 2023; Accepted: July 29, 2023

In this study, scaffolds whose main phase is an icosahedral quasicrystal (i-QC) were prepared for the first time by dynamic freeze-casting. Two different metal powders were used here, namely pure aluminum and quasicrystalline particles from the Al-Cu-Fe system. These powers were initially mixed with deionized water, citric acid, and poly(vinyl alcohol). The obtained slurry was frozen while rotating and freeze-dried under vacuum. The green bodies were subsequently heat-treated in a reducing atmosphere. The total porosity and mean pore size evaluated for these scaffolds were 62.4 ± 3.0% and 67.3 ± 2.8 μm, respectively. This is the first time that dynamic freeze-drying has been used in the preparation of QC scaffolds, which reinforces the novelty of this study. In addition, the proposed route is simple, inexpensive, and environmentally friendly, which is also worth highlighting.

Keywords: *Quasicrystals, Al-Cu-Fe system, Dynamic freeze-casting, Scaffolds, Structural characterization.*

1. Introduction

Freeze-casting is a promising approach for preparing samples with tailored pore structures[1-3]. This technique involves the controlled freezing of a liquid suspension, resulting in a scaffold-like structure characterized by a well-connected network of pores[4]. By adjusting the freezing parameters and the composition of the starting slurry, it is possible to control the size, shape, and orientation of the pore structure of the resulting material[5,6]. This makes freeze-casting an attractive option for many applications. An essential aspect of this technique is that the solvent used in the slurry acts as a sacrificial phase. During the subsequent sublimation step, the removal of the solvent leads to the formation of pores. As a consequence, freeze-casting can be classified as a space-holder process[7-9]. The use of water-based slurries in this study is noteworthy for several reasons. First, it significantly reduces both the cost and complexity of the process. In addition, it is consistent with environmentally friendly practices, as water serves as a benign and sustainable solvent. It is also worth noting that the use of freeze-casting can effectively reduce production costs compared to alternative methods such as rapid prototyping techniques (e.g. 3D printing)[10].

While the freeze-casting process was originally proposed for ceramic materials, its application has been extended to metallic materials in recent decades[11-13]. However, the use of metallic powders in freeze-casting presents a potential challenge related to particle settling. If the particles are dense or bulky, they may settle during the solidification step, resulting in undesirable density and porosity gradients in the final material[14]. To address this issue, a viable solution is to implement continuous agitation of the slurry during the freezing step, known as dynamic freeze-casting. This approach prevents the particles from settling before the slurry freezes, thus ensuring a uniform distribution of particles throughout the structure[15]. The use of dynamic freeze-casting makes it possible to produce porous materials even when working with dense starting materials, such as quasicrystalline particles.

Quasicrystals (QCs) have been widely studied over the past four decades due to their unique structural and physical properties[16,17]. Unlike ordinary crystals, which have periodic structures, QCs have structures with translational quasiperiodicity. As a result, they are composed of icosahedral, octagonal, decagonal, and dodecagonal units instead of the unit cells commonly observed in crystals[18]. QCs are commonly formed in binary, ternary, and quaternary systems, with Al-based alloys being the most commonly studied. The Al-Cu-Fe system is a notable QC system due to its low toxicity, high availability, and low cost[19,20]. In addition, the icosahedral quasicrystalline (i-QC) phase in this system has good stability and can be obtained by conventional processes[21]. One of the most important properties of QCs is their high hardness, which makes them suitable for use as cutting tools[22]. Other attractive properties of QCs are their high Young's modulus and superplasticity at high temperatures, which allow them to be used in structural applications where strength and stability are critical[23]. In addition to these promising mechanical properties, QCs also exhibit low coefficients of

*e-mail: witorw@demet.ufmg.br

friction and thermal conductivity. This makes them useful in a wide range of applications, from wear-resistant coatings to thermoelectric devices[21,24,25]. QCs have also found promising applications in catalysis due to the electronic nature and low surface energy of the quasicrystalline phases. In addition, many QCs systems contain catalytically active elements such as Cu and Pd in their composition[26]. Other potential uses include optics, sensing, energy storage, and thermal insulation[25,27,28]. It is worth noting that the properties of QCs are much closer to those of intermetallic compounds than to their metallic counterparts, making them particularly interesting from a practical perspective[19].

The preparation of porous samples has the potential to improve the use of QCs in various applications, primarily by increasing their surface area, light absorption, and insulating capacity. In particular, porous materials have a higher catalytic potential, which increases their effectiveness in catalysis. This enhanced catalytic behavior is due to the increased surface area as a result of the presence of pores in comparison to non-porous materials. It is noteworthy that we have not been able to find a substantial body of literature on the preparation of QC materials with significant porosity values. While there is existing research focusing on the formation of pores in QCs through leaching processes[29,30], our study stands out for its innovative approach. Our goal is to present a method for preparing scaffolds with high porosities in which the predominant phase is quasicrystalline. In doing so, we contribute to the advancement of knowledge in the field and pave the way for novel applications of QCs in the porous form.

2. Materials and Methods

2.1. Starting materials

The QC powder used in this work ($Al_{62.5}Cu_{25}Fe_{12.5}$) was prepared by gas atomization as described in detail elsewhere[31]. It has been reported that gas atomization of molten alloys is one of the technologies of material production that takes advantage of rapid solidification[32]. The QC powder was sieved to separate particle sizes in the range of 106 μm to 180 μm, and then ground by hand. Commercially pure aluminum (> 99.0%) was used in the sintering process. Deionized Milli-Q® water (H_2O), poly(vinyl alcohol) (PVA, Aldrich, M_w = 89,000-98,000 g.mol^{-1}, 99% hydrolyzed), and citric acid (CA, Aldrich, ≥ 99.5%) were also employed.

2.2. Freeze-cast scaffolds

QC and Al powders were initially mixed under stirring at room temperature with H_2O, PVA, and CA. The loading of metal powder (QC+Al) in these slurries was adjusted to 30 vol.%, while the concentrations of CA and PVA were kept at 1 wt.% and 5 wt.%, respectively. CA and PVA acted as a dispersant and a binder, respectively. The amount of Al added to the slurry was 15 vol.% of the metal powder, which represents 4.5% of the total volume. As will be discussed later, Al played a key role in the liquid phase-assisted sintering that occurred during the heat treatment step. The prepared slurries were poured into cylindrical polylactic acid molds, each with 30 mm high and 14 mm in diameter. The bottom side of these molds was made of conductive material (aluminum) to favor heat exchange with the environment. These molds were then transferred to a commercial freezer kept at about 15 °C for 24 h. They were continuously rotated at a speed of 25 rpm while in the freezer. The frozen samples were freeze-dried at -50 °C and 2.7×10^4 bar for 24 h on a Liotop L101 freeze-dryer. The green bodies were subsequently heat-treated at 800 °C for 6 h in a reducing atmosphere (95% N_2 + 5% H_2). Figure 1 shows the setup used for dynamic freeze-casting of the scaffolds prepared here.

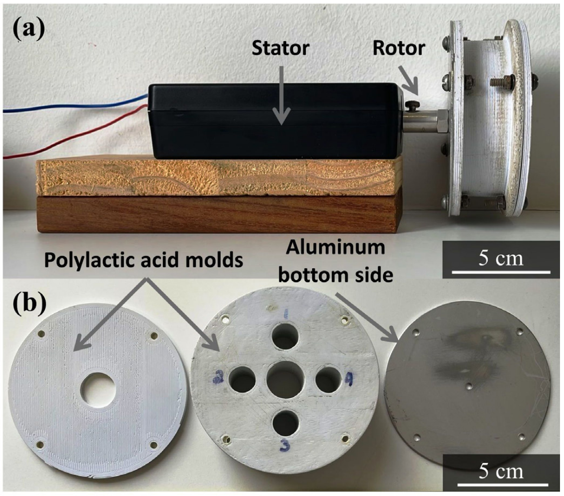

Figure 1. System used for freezing step while the slurry was in constant rotation: (a) side view of the system, and (b) polylactic acid mold and the aluminum base plate.

2.3. Characterizations

X-ray powder diffraction (XRD) was conducted on a Phillips-Panalytical PW-1710 diffractometer at a step size of 0.02° and using CuK_α as the radiation source (λ = 1.54 Å). Scanning electron microscopy was carried out on a Jeol JSM 5510 microscope at an accelerating voltage of 15 kV. In these tests, secondary electron (SE) and backscattered electron (BE) images were taken. Composition maps were collected by energy-dispersive X-ray spectroscopy (EDS) at an accelerating voltage of 15 kV on an Oxford Instruments Xmax EDX system coupled to a Jeol JSM-6360LV electron microscope. Laser granulometry was conducted on a Cilas 1064 analyzer using water as the dispersing medium and Triton X-100® (1 wt.%) as the dispersant. X-ray microtomography (microCT) was performed on a Bruker SkyScan 1174 system at an X-ray voltage of 50 kV. The pixel size used in these tests was about 20 μm. The mean pore size and porosity of the samples were evaluated using micro-CT, with hundreds of slices taken into account in these calculations. This sampling approach ensured a comprehensive evaluation and allowed for a representative calculation of these parameters. The values presented in this work reflect the mean ± standard deviation of the measurements for each sample.

3. Results and Discussion

The mean particle size evaluated by laser granulometry for the QC and Al powders were 69.0 μm and 79.9 μm, respectively. As displayed in Figures 2a and 2b, the Al particles have smooth surfaces while the QC powder has sharp edges. This behavior can be attributed to the hand milling step that QC underwent after atomization. Figure 2c exhibits XRD patterns taken for both metals. QC is composed of two phases, namely icosahedral quasicrystal (i-QC) and an Al-Cu solid solution (τ-AlCu(Fe)). The only phase detected for the Al powder was aluminum (α-Al). Figures 3a and 3b show, respectively, a digital photograph and a micro-CT model obtained for the scaffolds prepared here. The prepared cylindrical samples are approximately 3 cm in height and 1 cm in diameter. Figure 3c displays the pore size distribution evaluated for these materials. The total porosity and mean pore size of these specimens are 62.4 ± 3.0% and 67.3 ± 2.8 µm, respectively. It is worth mentioning that the closed porosity was negligible, revealing that a highly interconnected three-dimensional pore structure was obtained. These specimens could be handled without losing their integrity, indicating good mechanical stability. Preliminary tests conducted by sintering solely QC particles showed that the prepared scaffolds were fragile and crumbled upon handling, suggesting that this alloy has poor sinterability. Therefore, Al was added to the initial slurry to allow liquid phase-assisted sintering to take place and improve the efficiency of the heat treatment step.

Figures 4a and 4b exhibit low magnification cross-sectional and longitudinal SE micrographs of the scaffolds prepared here. A center-to-surface pore orientation is observed in Figure 4a, indicating that the ice front formed during freezing was able to push the metal particles without entrapment. Particle engulfment is commonly observed when freeze-casting is performed at high freezing rates on metal particles with micro-sized dimensions, which inhibits pore alignment[1,33]. In this work, the slurries were kept at 15 °C to allow a slow freezing rate of water and favor the growth of ice crystals. It is well established that nucleation is favored over growth for small freezing rates[34]. These ice crystals were removed during freeze-drying, leading to aligned pores in the prepared samples. In addition, the use of dynamic freeze-casting inhibits particle settling during the freezing process, which also contributes to the formation of a homogeneous pore structure. This approach has been employed in the preparation of Ti scaffolds for bone tissue engineering[15]. In this work, we report for the first time the use of this route for the preparation of QC scaffolds, which reinforces its novelty.

Figure 4c depicts the SE micrograph of the region highlighted in Figure 4b. Table 1 provides the chemical composition of points 1 to 6 displayed in Figure 4c. Figure 4d shows a typical XRD pattern of the scaffolds prepared here. The main phases detected by XRD and EDS were iQC, ω-Al_7Cu_2Fe, θ-Al_2Cu, τ-AlCu(Fe), and α-Al. The high concentration of Cu in point 5 may be due to the precipitation of θ-Al_2Cu[35]. This diversity of phases reveals that the QC and Al powders reacted during sintering. For instance, ω-Al_7Cu_2Fe has been reported to be derived from such a reaction[21]. Figures 5a and 5b show high magnification BE micrographs of the sintered scaffolds. Table 2 summarizes the chemical composition and space group of the phases detected in the prepared scaffold.

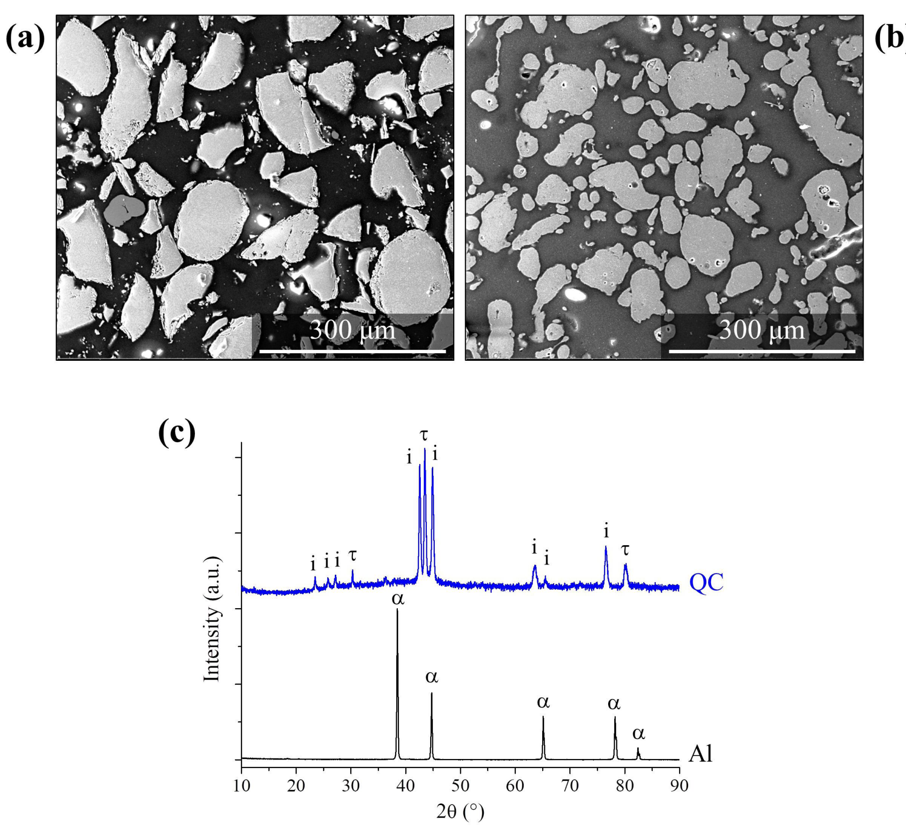

Figure 2. SEI micrographs of (a) QC and (b) Al particles, and (c) XRD patterns of these powders.

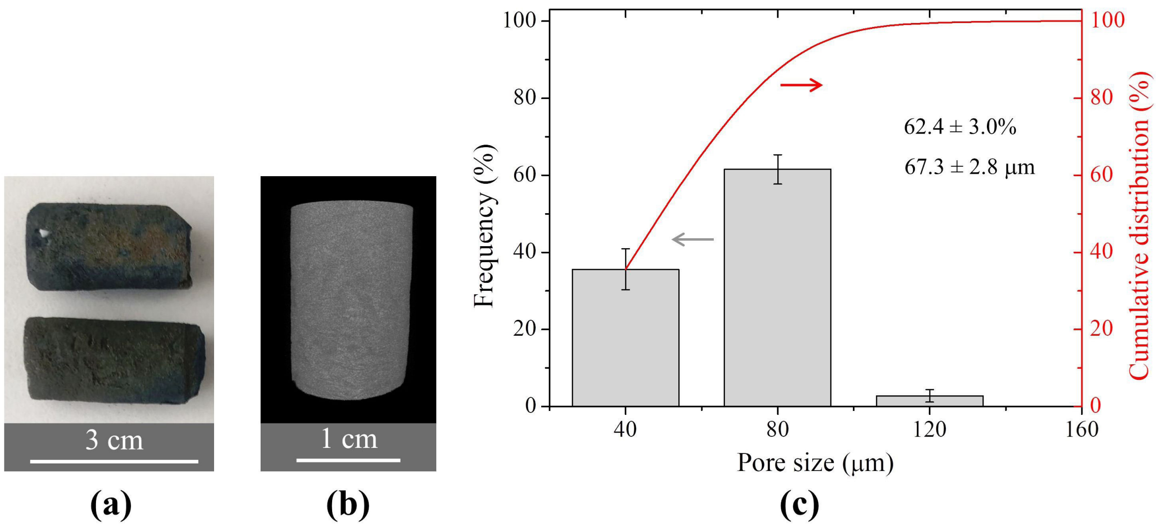

Figure 3. (a) Digital photograph of the samples produced, (b) 3D micro-CT image of an obtained scaffold, and (c) Pore size distribution evaluated by micro-CT for the scaffolds prepared in this study.

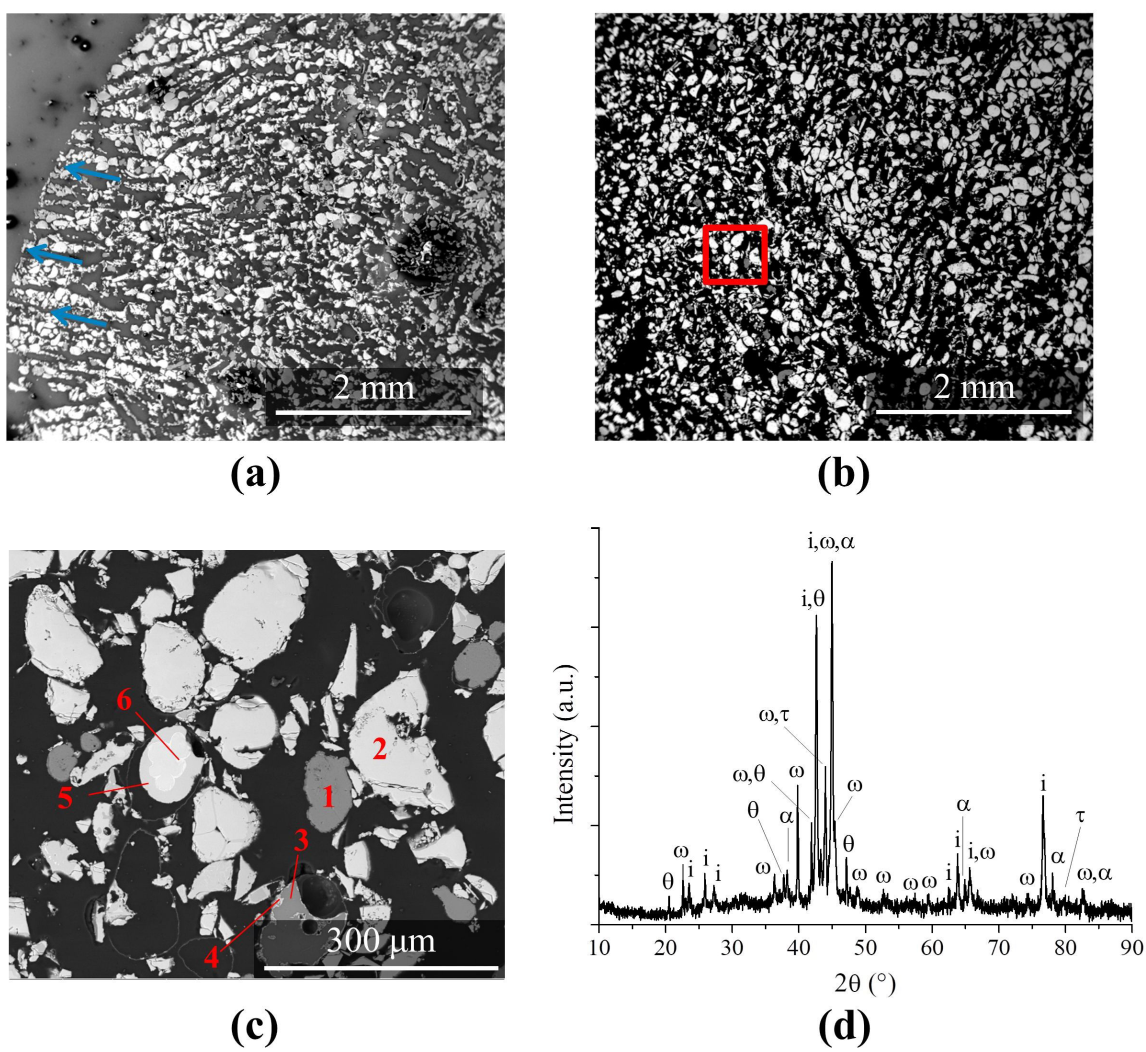

Figure 4. (a) Cross-sectional and (b) longitudinal SE images, (c) BE image of the region highlighted in (b), and (d) a typical XRD pattern taken for the prepared scaffolds.

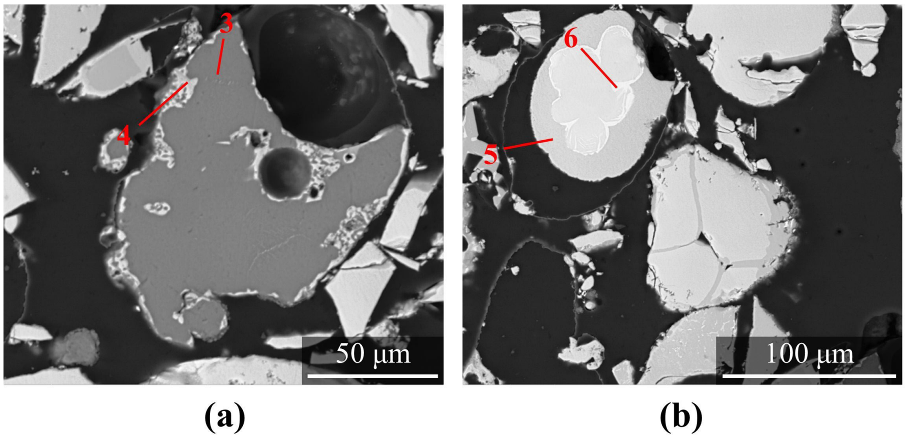

Figure 5. High magnification BE images of regions 3-4 (a) and 5 (b) shown in Figure 4c.

Table 1. Chemical composition and crystalline phases observed in the regions highlighted in Figure 4c.

Region	Crystal phase	Element (at.%)		
		Al	Cu	Fe
1	α	99.1	0.6	0.3
2	i	64.5	23.3	12.2
3	α	97.9	1.9	0.2
4	ω	73.2	20.6	6.2
5	θ	67.5	32.0	0.5
6	τ	52.0	47.2	0.8

Table 2. Chemical composition and space group of the phases observed in the microstructure of the prepared scaffolds.

Phase	Chemical composition	Space Group
α	Al	Fm$\bar{3}$m (22)
i	Al62,5Cu25Fe12,5	m$\overline{35}$ (23,24)
ω	Al7Cu2Fe	P4/mnc (25)
θ	Al2Cu	I4/mcm (26)
τ	AlCu(Fe)	Pm $\bar{3}$ m (26,27)

The preparation of porous samples from the QC powder of an Al-Cu-Fe alloy opens up new possibilities for using these materials in a range of applications, including catalysis, optics, gas/energy storage, membranes, optics, sensing, and thermal insulation. Porous QC samples are typically obtained by a leaching approach, which can be time-consuming, complex, and environmentally unfriendly due to the use of toxic reagents[29,36]. As an example, Mishra et al.[29] obtained a porous alloy of the Al-Cu-Fe system by promoting the leaching of a bulk sample with an aqueous NaOH solution. Although the resulting samples were able to promote the degradation of methylene blue in water, their preparation required leaching times of up to 8 h. The route used here is straightforward, allowing the preparation of samples with porosities above 60% and with homogeneous pores. This porosity can be tailored by adjusting conditions such as the volume fraction of metal powder added to the initial slurry, the freezing rate, and the freezing vehicle. Furthermore, the use of low-toxicity and environmentally fiendly reagents in this work such as water, citric acid, and poly(vinyl alcohol) should be highlighted. This strategy has several benefits, including health and safety, as the use of low-toxicity reagents reduces the risk of workers being exposed to harmful chemicals; environmental protection, as many chemicals used in laboratories, can be harmful to the environment, causing pollution and disrupting ecosystems; and cost savings, as green reagents can be less expensive than traditional chemicals because they can be produced using more sustainable methods and may require less energy to produce and dispose of.

4. Conclusions

In this work, QC scaffolds were successfully produced by dynamic freeze-casting. Al powder was used to promote liquid-phase-assisted sintering and improve the effectiveness of the heat treatment step. The total porosity and mean pore size of these scaffolds were 62.4 ± 3.0% and 67.3 ± 2.8 µm, respectively. It was observed that QC and Al powders reacted during the sintering step, resulting in different phases, including iQC, ω-Al_7Cu_2Fe, θ-Al_2Cu, τAlCu(Fe), and α-Al. The use of dynamic freeze-casting allowed the preparation of samples with homogeneous pore structures by preventing the metal particles from settling in the starting slurry. These materials, which can be handled without crumbling, can be used in many applications and are of technological interest.

5. Acknowledgements

The authors thank the financial support from FAPEMIG (APQ-00762-21), CNPq (306193/2020-5, 403191/2021-1, and 304415/2021-9), FAPESP, and CAPES (PROEX). The authors are grateful for technical support from UFMG and UFSCar. The authors also thank Prof. Walter José Botta and Prof. Claudemiro Bolfarini for providing the Al-Cu-Fe powder.

6. References

1. Deville S. Freeze-casting of porous ceramics: a review of current achievements and issues. Adv Eng Mater. 2008;10(3):155-69.
2. Thongprachan N, Nakagawa K, Sano N, Charinpanitkul T, Tanthapanichakoon W. Preparation of macroporous solid foam from multi-walled carbon nanotubes by freeze-drying technique. Mater Chem Phys. 2008;112(1):262-9.

3. Chen H, Ma Y, Lin X, Yang D, Chen Z, Li X, et al. Preparation of aligned porous niobium scaffold and the optimal control of freeze-drying process. Ceram Int. 2018;44(14):17174-9.
4. Chen HM, Yin YF, Dong HB, Tong Y, Luo M, Li X. Porous alumina infiltrated with melt and its dynamic analysis during pressureless infiltration. Ceram Int. 2014;40(4):6293-9.
5. Deville S. Ice-templating, freeze casting: beyond materials processing. J Mater Res. 2013;28(17):2202-19.
6. Zuo KH, Zeng YP, Jiang D. Properties of microstructure-controllable porous yttria-stabilized zirconia ceramics fabricated by freeze casting. Int J Appl Ceram Technol. 2008;5(2):198-203.
7. Atwater MA, Guevara LN, Darling KA, Tschopp MA. Solid state porous metal production: A review of the capabilities, characteristics, and challenges. Adv Eng Mater. 2018;20(7):1-33.
8. Saheban M, Bakhsheshi-Rad HR, Kasiri-Asgarani M, Hamzah E, Ismail AF, Aziz M, et al. Effect of zeolite on the corrosion behavior, biocompatibility and antibacterial activity of porous magnesium/zeolite composite scaffolds. Mater Technol. 2019;34(5):258-69.
9. Karadeniz Ş, Arslan E. Microstructural characterization and wear behavior of porous equimolar TiNbZr medium-entropy alloys scaffolds produced by mechanical alloying. Mater Res. 2022;25:1-7.
10. Singh R, Lee PD, Dashwood RJ, Lindley TC. Titanium foams for biomedical applications: a review. Mater Technol. 2010;25(3-4):127-36.
11. Scotti KL, Dunand DC. Freeze casting: a review of processing, microstructure and properties via the open data repository, FreezeCasting.net. Prog Mater Sci. 2018;94:243-305.
12. Bakhsheshi-Rad HR, Hamzah E, Staiger MP, Dias GJ, Hadisi Z, Saheban M, et al. Drug release, cytocompatibility, bioactivity, and antibacterial activity of doxycycline loaded Mg-Ca-TiO_2 composite scaffold. Mater Des. 2018;139:212-21.
13. Dayaghi E, Bakhsheshi-Rad HR, Hamzah E, Akhavan-Farid A, Ismail AF, Aziz M, et al. Magnesium-zinc scaffold loaded with tetracycline for tissue engineering application: in vitro cell biology and antibacterial activity assessment. Mater Sci Eng C. 2019;102:53-65.
14. Chino Y, Dunand DC. Directionally freeze-cast titanium foam with aligned, elongated pores. Acta Mater. 2008;56(1):105-13.
15. Do Jung H, Yook SW, Jang TS, Li Y, Kim HE, Koh YH. Dynamic freeze casting for the production of porous titanium (Ti) scaffolds. Mater Sci Eng C. 2013;33(1):59-63.
16. Dubois J. So useful, those quasicrystals. Isr J Chem. 2011;51(11–12):1168-75.
17. Mukhopadhyay NK, Yadav TP. Quasicrystals: a new class of structurally complex intermetallics. J Indian Inst Sci. 2022;102(1):59-90.
18. Sordelet DJ, Dubois JM. Quasicrystals: perspectives and potential applications. MRS Bull. 1997;22(11):34-9.
19. Huttunen-Saarivirta E. Microstructure, fabrication and properties of quasicrystalline Al−Cu−Fe alloys: a review. J Alloys Compd. 2004;363(1–2):154-78.
20. Travessa DN, Cardoso KR, Wolf W, Junior AMJ, Botta WJ. The formation of quasicrystal phase in Al−Cu−Fe system by mechanical alloying. Mater Res. 2012;15(5):749-52.
21. Dubois JM. Properties- and applications of quasicrystals and complex metallic alloys. Chem Soc Rev. 2012;41(20):6760-77.
22. Inoue A. Bulk amorphous and nanocrystalline alloys with high functional properties. Mater Sci Eng A. 2001;304–306:1-10.
23. Ustinov AI, Polishchuk SS, Skorodzievskii VS, Bliznuk VV. Effect of grain size on the damping capacity of quasicrystalline Al−Cu−Fe materials. Surf Coat Tech. 2008;202(24):5812-6.
24. Dubois JM. New prospects from potential applications of quasicrystalline materials. Mater Sci Eng A. 2000;294–296:4-9.
25. Wolf W, Schulz R, Savoie S, Bolfarini C, Kiminami CS, Botta WJ. Structural, mechanical and thermal characterization of an Al−Co−Fe−Cr alloy for wear and thermal barrier coating applications. Surf Coat Tech. 2017;319:241-8.
26. Tanabe T, Kameoka S, Tsai AP. Microstructure of leached Al−Cu−Fe quasicrystal with high catalytic performance for steam reforming of methanol. Appl Catal A Gen. 2010;384(1-2):241-51.
27. Wolf W, Bolfarini C, Kiminami CS, Botta WJ. Recent developments on fabrication of Al-matrix composites reinforced with quasicrystals: from metastable to conventional processing. J Mater Res. 2021;36(1):281-97.
28. Verma SK, Bhatnagar A, Shaz MA, Yadav TP. Mechanistic understanding of the superior catalytic effect of $Al_{65}Cu_{20}Fe_{15}$ quasicrystal on de/re-hydrogenation of NaAlH4. Int J Hydrogen Energy. 2022
29. Mishra SS, Yadav TP, Singh SP, Singh AK, Shaz MA, Mukhopadhyay NK, et al. Evolution of porous structure on Al–Cu–Fe quasicrystalline alloy surface and its catalytic activities. J Alloys Compd. 2020;834:155162.
30. Zhang F, Guo H, Wang L, Ma H, Li H, Zhang L, et al. Porous $Al_{63}Cu_{25}Fe_{12}$ quasicrystals covered with $(Al_{11.5}Fe_{13.9}Cu_{19.7})O_{54.9}$ nanosheets. Mater Charact. 2019;147:165-72.
31. Wolf W, Koga GY, Schulz R, Savoie S, Kiminami CS, Bolfarini C, et al. Wear and corrosion performance of Al−Cu−Fe−(Cr) quasicrystalline coatings produced by HVOF. J Therm Spray Technol. 2020;29:1195-207.
32. Grgač P, Behúlová M, Moravčík R, Mesárošová J. Gas atomization of molten alloys is one of the technologies of material production that takes advantage of rapid solidification. Mater Res. 2012;15(5):705-12.
33. Du W, Yao Z, Moliar O, Tao X, Zhang Q, Loboda P, et al. Fabrication and compressive properties of directional porous titanium scaffold by freeze casting TiH_2 powders. J Alloys Compd. 2022;894:162363.
34. Deville S, Saiz E, Tomsia AP. Freeze casting of hydroxyapatite scaffolds for bone tissue engineering. Biomaterials. 2006;27(32):5480-9.
35. Wolf W, Bolfarini C, Kiminami CS, Botta WJ. Fabrication of Al-matrix composite reinforced with quasicrystals using conventional metallurgical fabrication methods. Scr Mater. 2019;173:21-5.
36. Pandey SK, Bhatnagar A, Mishra SS, Yadav TP, Shaz MA, Srivastava ON. Curious catalytic characteristics of Al−Cu−Fe quasicrystal for de/rehydrogenation of MgH_2. J Phys Chem C. 2017;121(45):24936-44.